SQT

SCIENCE APPLICATIONS Incorporated

(NASA-CR-161687) A SURVEY OF SPACE RADIATION EFFECTS (Science Applications, Inc., Huntsville, Ala.) 31 p HC A03/MF A01 CSCL 03B

N81-23006

Unclas

G3/93 21595

SAI-81-555-HU

A SURVEY OF

SPACE RADIATION EFFECTS

Contract No. NAS8-32387

Space Base Radiation Analysis Study

Prepared by:

C. W. Hill

Prepared for:

George C. Marshall Space Flight Center
Marshall Space Flight Center, Alabama 35812

March 18, 1980

SCIENCE APPLICATIONS, INC.

2109 W. Clinton Avenue, Suite 800
Huntsville, Alabama 35805 (205) 533-5900

FOREWORD

This report is submitted in accordance with the requirements of Contract NAS8-32387. The Contract Officer's Representative is John W. Watts, Space Sciences Laboratory, George C. Marshall Space Flight Center, Alabama 35812.

TABLE OF CONTENTS

1. INTRODUCTION

As NASA space missions increase in scope, duration, and complexity, the effects of space radiation upon those missions become more significant. The type of radiation hazard may depend on location; i.e., the Jupiter radiation belts or a solar explorer. Alternatively the hazard may depend on special equipment used such as a star tracker with a fluorescing faceplate or a computer with submicron circuit geometry. It is increasingly necessary to search for potential radiation problems in the design stage of a mission. This report is intended to acquaint non-nuclear personnel with some of the potential problem areas.

Section 2 discusses radiation damage to solar cells and the revolutionary advances being made.

Section 3 examines radiation effects to electronics components other than solar cells, and Section 4 explores several specialized areas such as radioactivity and luminescence.

2. SOLAR CELLS

Solar cell arrays have provided power on the majority of space missions, particularly for long-duration flights. The radiation damage to solar cells has been measured in low earth orbit and geosynchronous orbit.

The design of efficient, radiation-resistant solar cells progressed slowly from about 1962 to 1972. The state-of-the-art at the end of that period is summarized in "The Solar Cell Radiation Handbook" (Ref. 1). The Comsat violet cell had just been introduced (Ref. 2) and other improvements were vigorously developed over the next five years. Today, the solar cell technology is changing so rapidly that a cell design is often outmoded by the time it can be space qualified. For this reason it is difficult to project solar cell characteristics more than a very few years into the future. Further, questions dealing with methods of improving the radiation resistance of Ga As (galium arsenide) cells are only now beginning to be addressed. Certain features of the new silicon and Ga As technologies will be outlined in this report.

Because the solar cell is a device with complex behavior, a variety of methods are available to measure radiation damage. The commonly used measures include open circuit voltage, short circuit current, maximum power output, and diffusion length damage coefficient. The first three may be understood by referring to Figure 2-1, which shows I-V (current voltage) curves for a typical space-qualified commercial solar cell and a Comsat violet cell before and after irradiation. For the violet cell, the open circuit voltage at zero current falls from 595 mV to about 570 mV after irradiation to 3×10^{14} e/cm^2. The short circuit current at zero voltage falls from 160 mA to 142 mA after irradiation. These two data points are easy to measure. The maximum power is determined by detailed measurements near the knee of the I-V curve. In Figure 2-1 it lies at the point of highest efficiency. The violet cell falls from 13.7 to 11.7 percent efficiency after irradiation.

The damage mechanism to the bulk of the solar cell is the creation of dislocation sites in the crystalline lattice. These sites serve as recombination centers for holes and electrons, which shorten the diffusion length and act as an internal short circuit. The minority carrier diffusion length, L,

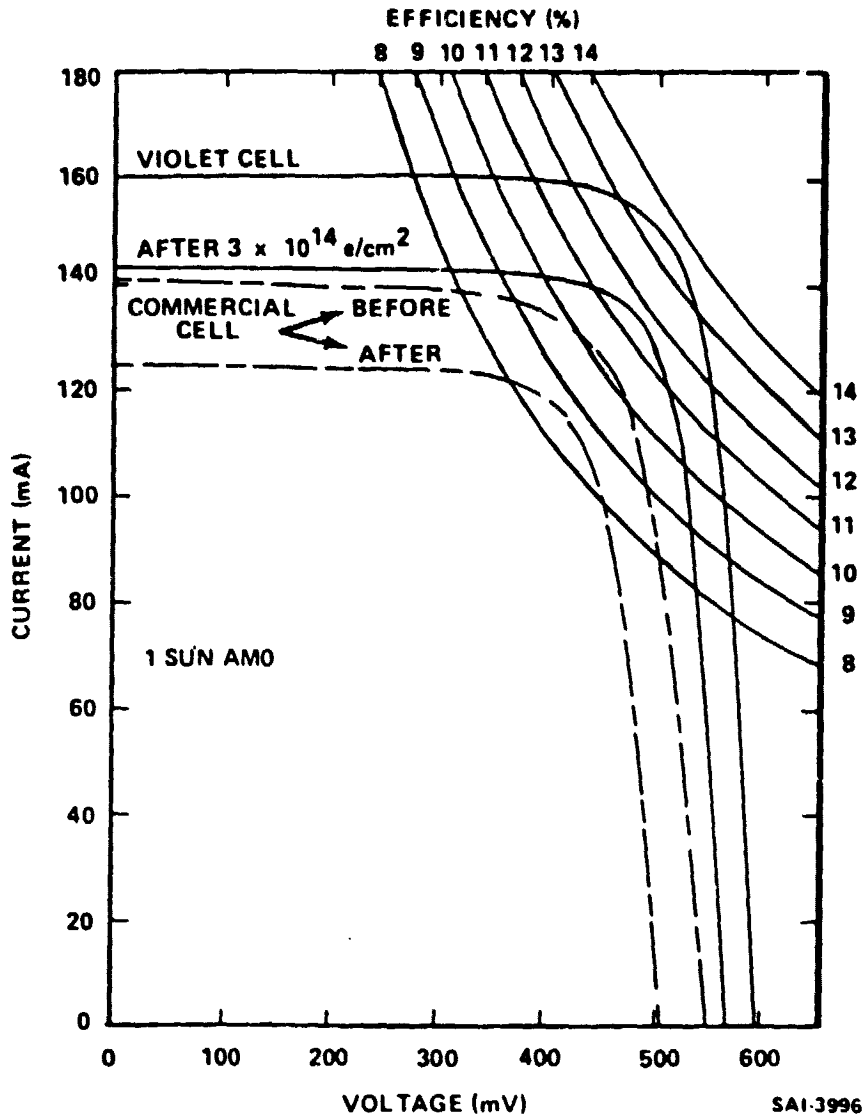

Figure 2-1. I-V Curves for a Violet Cell and a Commercial Cell before and after Irradiation by 3×10^{14} e/cm^2 (Ref. 2)

and its initial value, L_0, are related by the following equation at a standard temperature.

$$\frac{1}{L^2} = \frac{1}{L_0^2} + K\,\phi$$

Here ϕ is the fluence, often expressed in equivalent 1 MeV electrons, and K is the damage coefficient. This damage coefficient is a function of the particle type and energy as well as the base material and impurities. Figure 2-2 shows electron damage coefficients for several n/p cells. Protons are more effective than electrons in creating lattice defects due to their larger mass. The I-V curves may be constructed from material parameters, radiation exposure, and damage coefficients.

Radiation damage to solar cells may be reduced in several ways. One way is to coat the cells with a cover glass layer to shield out low energy protons and electrons. Figure 2-4 shows early data on the effect of cover slides at extending lifetimes in various orbits. Care must be taken in choosing cover materials and adhesives so that exposure to particulate radiation and light do not reduce light transmission due to discoloration.

Another way to improve the radiation resistance of a solar cell is to load it with certain impurities, such as lithium, which will migrate to defect sites and neutralize them as recombination centers.

The Comsat violet cell has a shallow junction. Ultraviolet light that would normally be absorbed and lost in front of the junction is utilized to generate charge carriers, thus extending the spectral response and raising the efficiency. The short wavelength light produces carriers near the junction, so the uv response should be less affected by radiation-induced defects than other portions of the spectrum.

The Comsat violet cell has a high efficiency (13.7 percent from Figure 2-1). This response is achieved by diffusing fewer impurities into the surface junction, thus reducing the dead layer and permitting blue light to get into the active region. However, this approach does not reduce the bulk material radiation damage, and the reduction in efficiency of both the violet cell and commercial cell during a test was the same (14.5 percent) due to the irradiation.

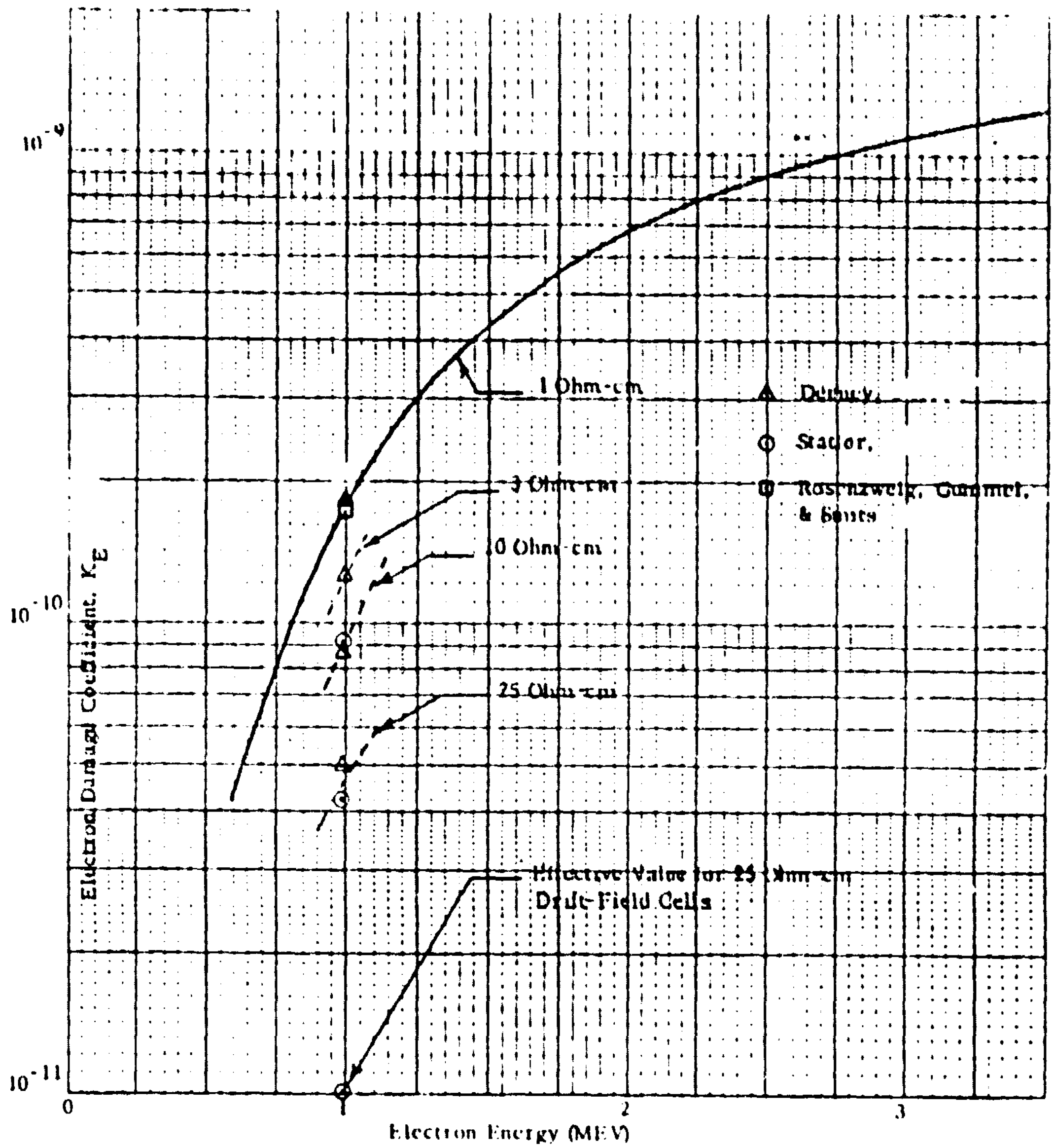

Figure 2-2. Electron Damage Coefficient as a Function of Electron Energy for N/P Silicon Cells (Ref 3)

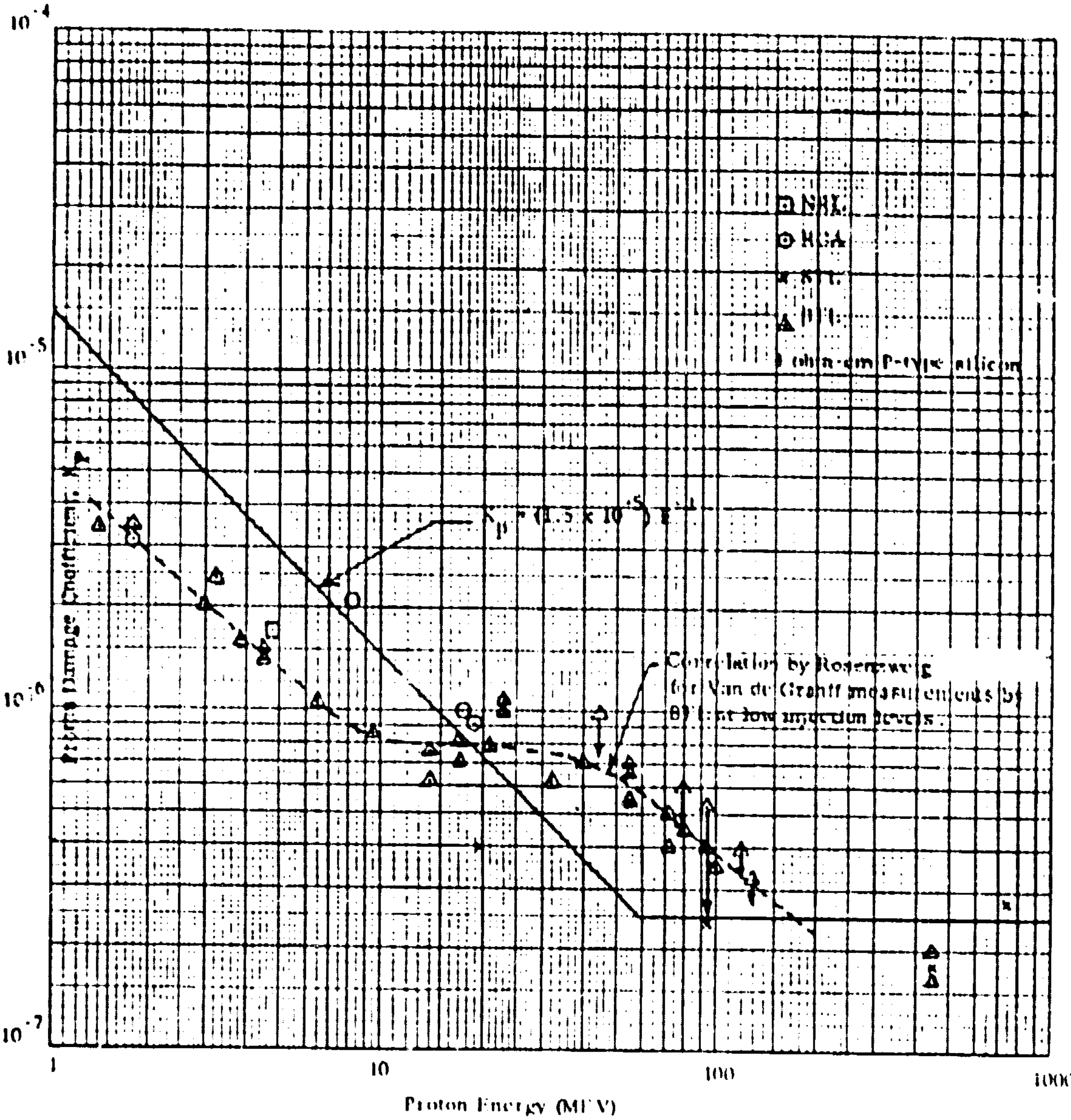

Figure 2-3. Proton Damage Coefficient for N/P Silicon Cells as a Function of Proton Energy (Ref 3)

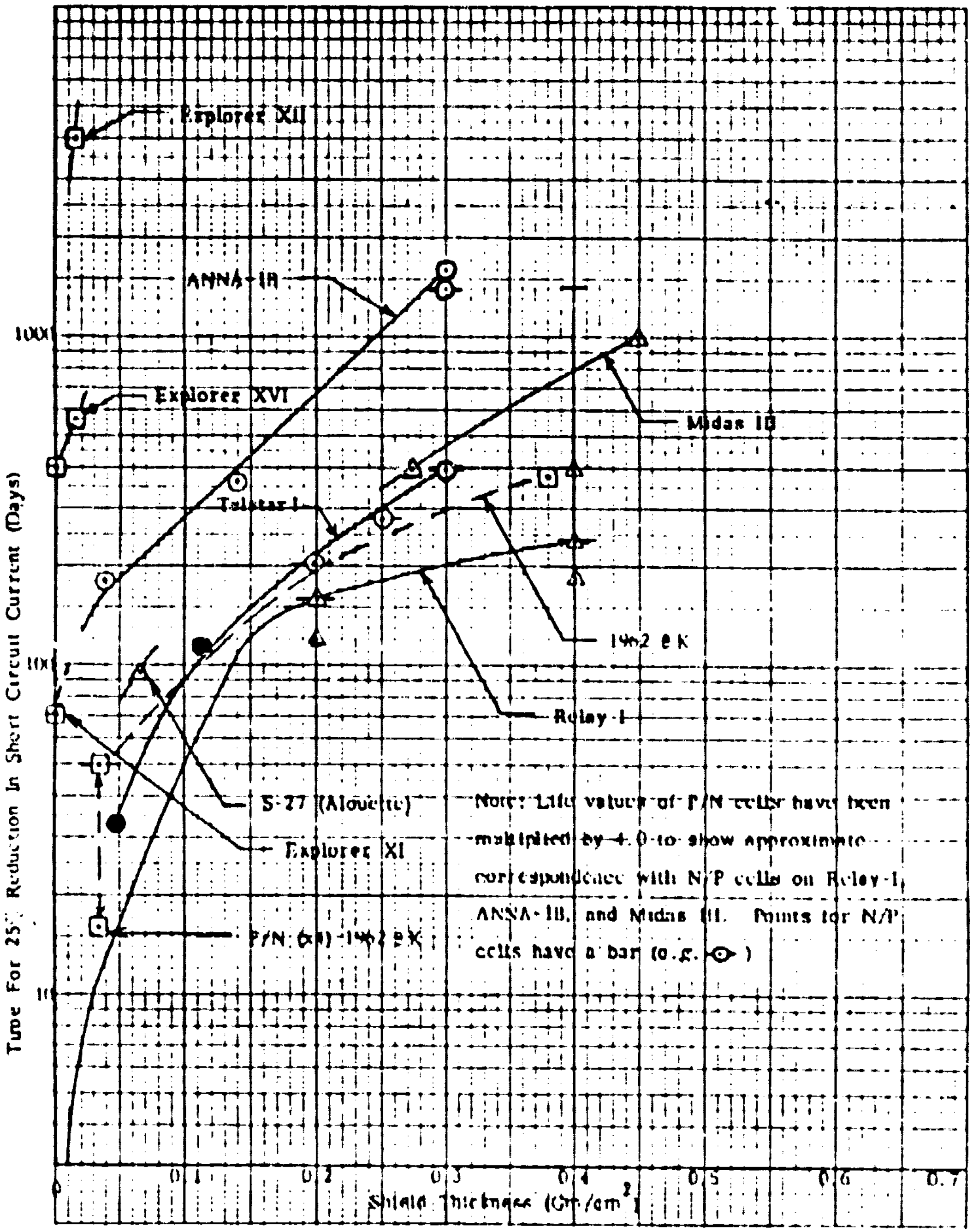

Figure 2-4. Composite Graph of Life of Silicon Solar Cells vs Shield Thickness for Various Orbits (Ref 3)

Another method of increasing efficiency is illustrated in Figure 2-5 (Ref 4) A cover slide with a sawtooth surface is placed over the cell. Parallel light incident on the slide is refracted as shown in Figure 2-5a. The shaded diamond-shaped areas represent regions where light incident along the normal does not penetrate. The periodicity and phase of the sawtooth pattern may be chosen to put the collection grids in shadow, which reduces by half or more the 7 to 10 percent of incident light obstructed by conventional grid structures. The behavior is illustrated in Figure 2-5b and 2-5c for different cover glass thicknesses. A further claim for this concept is that reflected light is reduced by offering a second surface for reflected light to enter the cell. The normal 2 to 4 percent reflected component may be reduced to less than one percent in this way; reflection losses are stated to be less than those of an anti-reflection coating on a plane surface. If the sawtooth cover slide can be combined with wrap-around grids (where the fine grid lines continue over the edge to the back side for collection), the contact and grid obstruction losses can be reduced to zero and reflection losses to less than one percent. The potential improvement in efficiency is 10 percent or more.

A third method for raising efficiency is utilization of the wrap-around grid mentioned above. Placement of the coarse collection grid bus bars on the back side reduces shadowing effects on active portions of the cell. This technique may not improve quoted cell efficiencies in some instances because shadowed areas are often subtracted before efficiency is computed.

The sawtooth cover slide and wrap-around grid do not improve solar cell radiation resistance except for bulk shielding effects. However, a higher initial efficiency leads to a higher end-of-life efficiency if other parameters are held constant.

In contrast, the vertical junction solar cell was proposed by Wise (Ref 5) and Rahilly (Ref 6) to reduce the effect of radiation upon solar cells. Vertical junctions are made possible because alkaline solutions etch silicon anisotropically under certain conditions. Etch rate differences of 400 to 1 have been obtained between the 110 plane and the 111 plane. Patterns are placed on the surface of aligned 110 wafers by photoresist techniques, then etching and junction diffusion are performed. Figure 2-6 shows the structure of a vertical junction cell developed by Lindmayer, Wrigley, and Wohlgemuth (Ref 7). The walls and

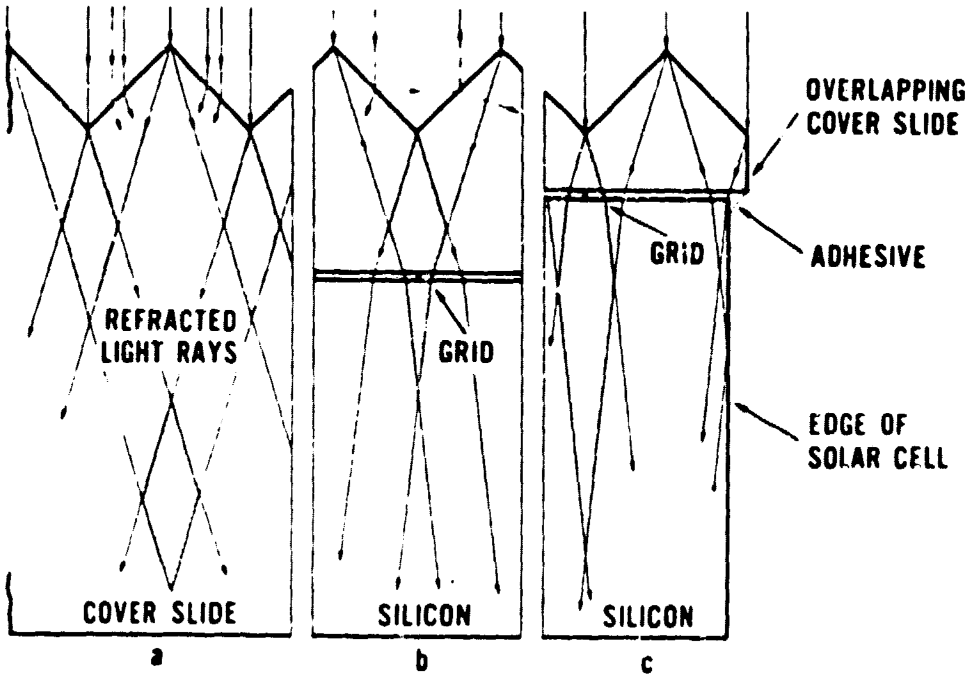

Figure 2-5. Structure and Effect of the Sawtooth Cover Slide (Ref 4)

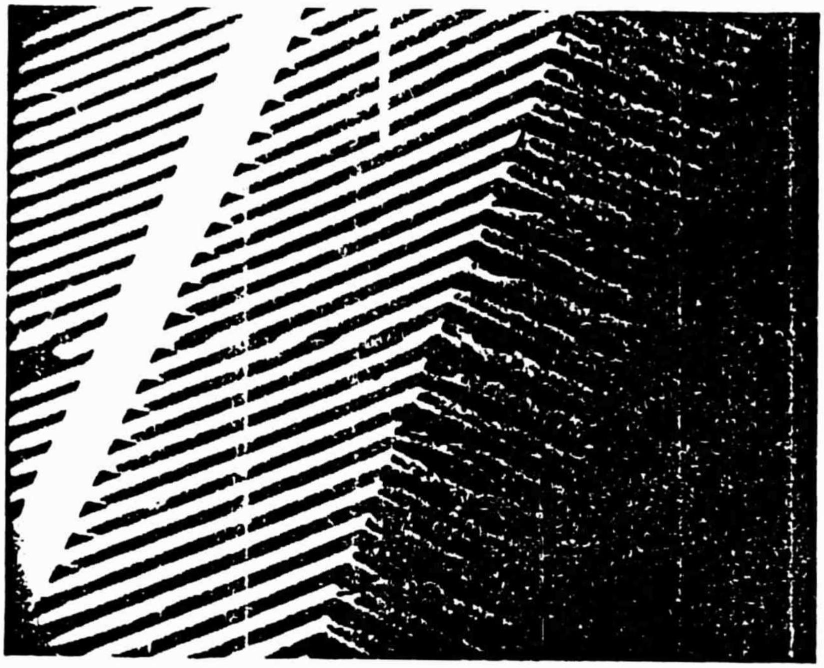

Figure 2-6. Scanning Electron Microscope Picture at a Magnification of 250 χ of a Vertical Junction Cell Broken Perpendicular to the Grooves (Ref 6)

ORIGINAL PAGE IS
OF POOR QUALITY

channels are generally 5 to 10 micrometers wide and 100 to 150 micrometers deep. Cells 2 cm by 2 cm have been manufactured; efficiencies over 13 percent have been obtained. Reflection losses are small and may be reduced further by tapering the etch.

The number of defect centers generated by radiation in vertical junction cells is about the same as in planar cells. The defects cause less degradation, however, because charge carriers generally have to travel only a few micrometers to reach a junction. Irradiation with one MeV electrons to accumulated fluences of 5.10^{15} per square centimeter produced only half the degradation that it did in similarly processed planar cells.

Back surface field (BSF) cells represent an attempt to increase efficiency by putting an additional collection junction on the back surface. Such cells usually have higher short circuit currents out to fluences of 10^{14} to 10^{15} e/cm^2. Above this point, the BSF cells revert to the behavior of shallow junction (violet) cells (Ref 8).

Gallium arsenide (Ga As) cells offer potentially higher efficiency than silicon cells. The technology status of Ga As cells appears to be that of 10 to 15 years ago for silicon cells. A rapid development pace based on an understanding of silicon behavior is probable. Very limited data indicate that early samples (not optimized against radiation) may be less vulnerable to neutrons but more vulnerable to electrons and protons than silicon cells (Ref 9).

In summary, silicon cells which used to have conversion efficiencies of 9 to 10 percent are now up to 14 percent in the preproduction stage and 15 percent for selected samples. The maximum achievable is 18 to 20 percent according to recent models. Radiation resistance of silicon cells has been increased greatly in recent years. A 20% degradation at 5.10^{15} e/cm^2 (1 MeV equivalent) is possible. Ga As cells have a theoretical efficiency limit of 26 percent, and have achieved 18.5 percent for small cells and 17 percent for large cells. A reasonable goal is about 22 percent. The radiation damage mechanisms in the more complicated Ga As cell structure are not well understood.

The high cost of solar cells suggests the possibility of using fewer cells in conjunction with collecting mirrors in a corrugated arrangement. This approach would cause the cells to operate at a higher temperature and reduce cumulative radiation damage because of annealing effects.

The fact of radiation damage to solar cells is accounted for in solar array design by oversizing the array. Accurate calculations and/or experimental data are necessary so that peak power demands are met over the mission duration witnout excessive weight penalties.

3. RADIATION EFFECTS TO ELECTRONICS

Solar cells and many kinds of detectors are solid state devices. Their uses are sufficiently specialized to warrant individual discussion in the previous section. This section will examine radiation damage to semiconductor devices normally found in electronic components.

An n-type material contains doping atoms which supply electrons for conduction. A p-type material contains doping atoms which absorb electrons from the lattice, leaving holes or positively charged regions. Given a potential difference, an electron from an adjacent lattice point may move to fill the hole. In effect, the hole has moved.

In a p-n junction, electrons thermally diffuse from the n-side to the p-side where they are called minority carriers. Similarly, holes diffuse to the n-side and become minority carriers there. Bulk radiation damage is related to interactions causing defects in the lattice structure. The defects serve as recombination sites for the minority carriers and shorten their lifetime. The result is decreased gain from transistors and decreased short circuit current and maximum power for solar cells. These bulk radiation damage effects are termed "permanent damage" though a portion of the damage can be removed by annealing.

Ionizing radiation can interact with atmosphere, passivation layers, and surface contaminants to change electric fields at junction surfaces and thus change surface recombination characteristics of the current carriers. These changes are often erratic from vendor to vendor, or even batch to batch.

Short term radiation effects can be caused by ionization processes that modify conduction currents. This effect at the base-emitter junction of a transistor may be amplified by the current gain. The dose rate required to induce this effect is typical of nuclear weapon bursts, but not of space radiation. For this reason, dose rate effects will not be examined in this section.

The wide variety of devices and technologies available today makes it difficult to predict radiation vulnerability without tests. Generally, MOS and CMOS FET's (field effect transistors) are nearly invulnerable to bulk displacement type damage but are quite sensitive to total ionization dose. On the other hand, bipolar components are relatively sensitive to bulk effects and usually less sensitive to ionization effects. Chips containing many planar devices are more sensitive than single components as a rule.

The annealing of radiation damage is possible at elevated temperatures over a period of time. The ionization damage to surface layers of planar silicon devices may often be healed by baking at 300° C for one hour. This behavior raises a question about low dose rates at moderate temperatures. If a certain dose delivered in a few minutes causes failure of a device at 20° C, could the device remain operational if the same dose were delivered over a longer time period, perhaps years? The answer is not known, and conservative practice will not rely on long-term annealing at moderate temperatures until tests confirm this behavior.

An occasional "maverick" transistor exhibits much greater sensitivity to radiation than similar devices from the same manufacturer, even those from the same batch. Figure 3-1 shows abnormal behavior for a 2N2222A PNP transistor (Ref. 10). Here, β_0 is the initial gain of the device. The shaded band shows minimum gain change at 10^4 rads with no bias applied and maximum collector current. The unshaded band shows slightly greater damage when bias is applied. One sample showed a much larger gain change than the others. After the damage was annealed out, a second irradiation to 10^4 rads caused similar damage. The damage could be healed because it is a surface effect which often shows up at much smaller (factor of 50) doses than bulk damage. It may be feasible, though expensive, to test all the transistors to be used in critical circuits for "maverick" behavior; a subsequent anneal could heal most of the damage.

The radiation sensitivity of various types of electronic components is shown in Figures 3-2 and 3-3 Figure 3-2 gives damage in terms of rads, usually rads silicon, for devices sensitive to ionizing radiation. Figure 3-3 shows damage regimes in terms of equivalent 1-MeV electrons/cm^2 and neutrons/cm^2 (E > 10 KeV).

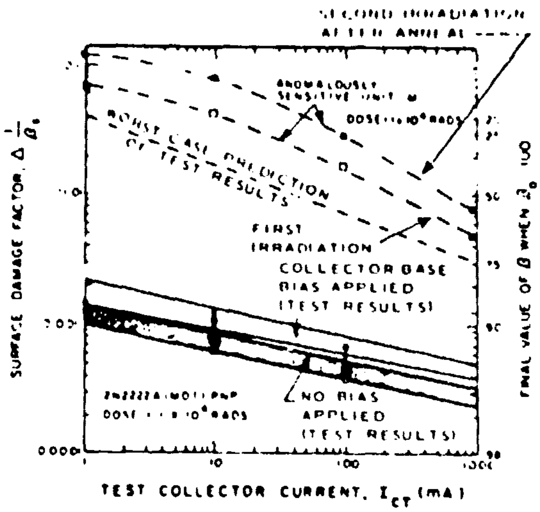

Figure 3-1. Result of Co^{60} Gamma Ray Irradiation of Motorola-Type 2N2222A Transistors (Damage vs Collector Current) (Ref 10)

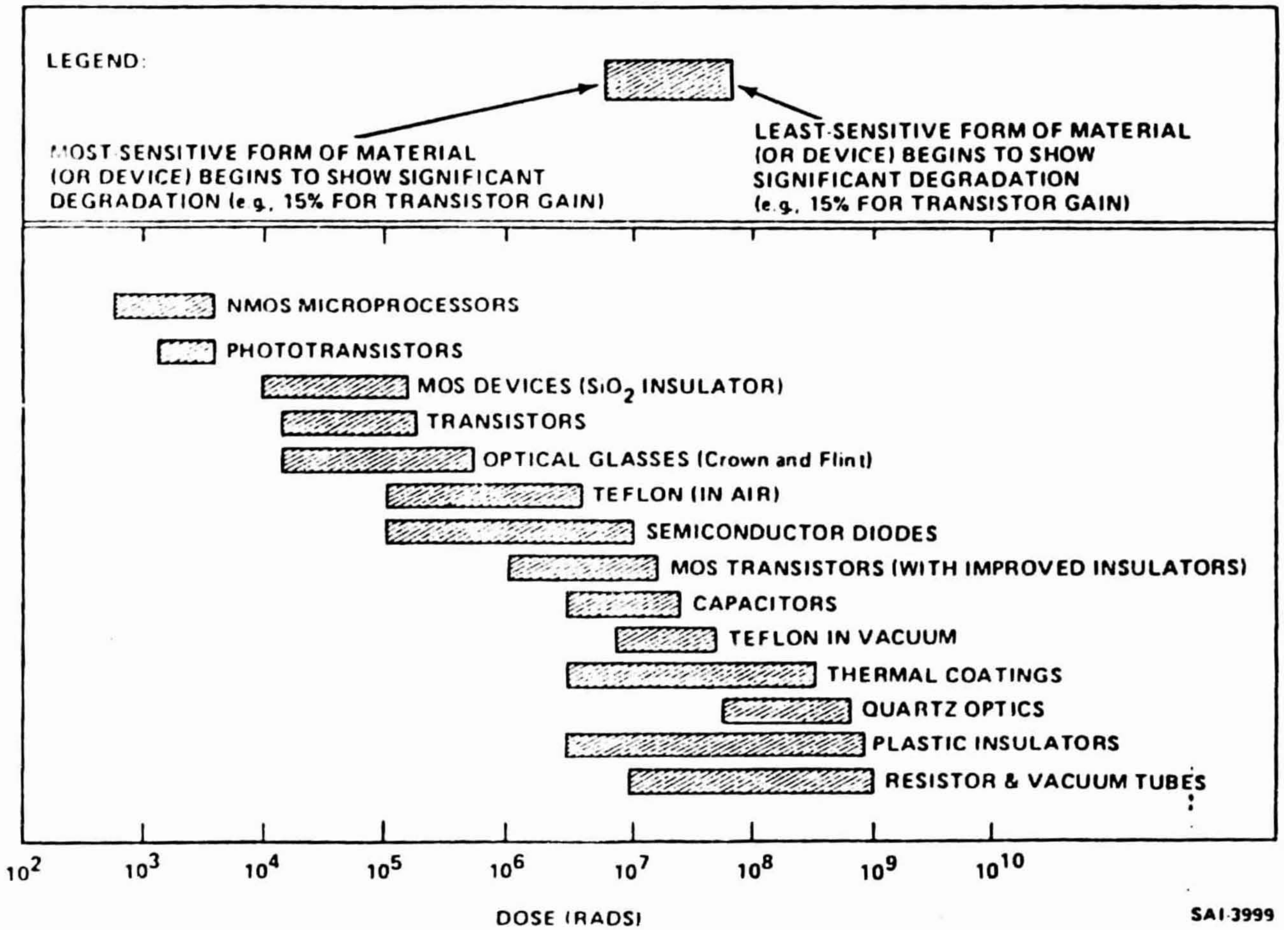

Figure 3-2. Sensitivity of Various Components to the Ionization Effects of Radiation (Ref 10)

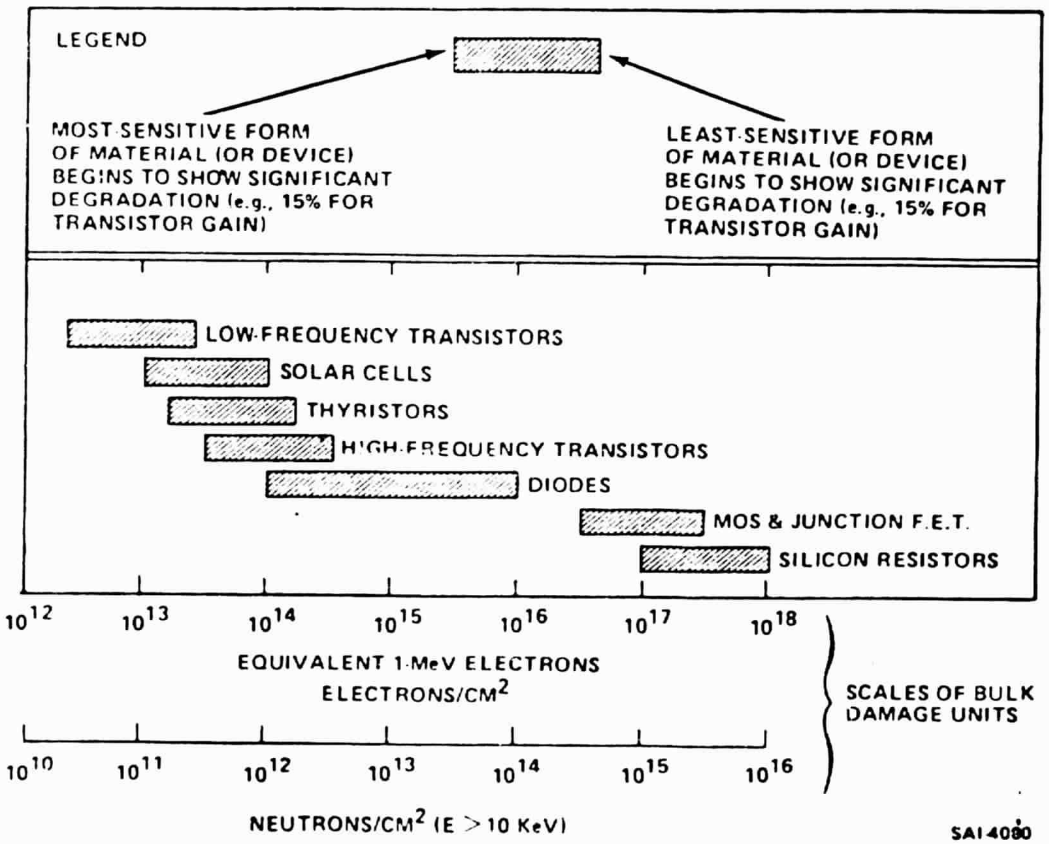

Figure 3-3. Sensitivity of Various Components to the Bulk Damage Effects of Radiation (Ref 10)

Other components such as optical glass, teflon, quartz, and thermal coatings are included in Figure 3-2 for completeness.

Generally, the more complex surface devices exhibit the least radiation tolerance. One type of microprocessor fails at only 500 rads. Another test of 5 processors from 6 manufacturers showed a damage threshold at 1000 rads and failure of all samples at 3000 rads (Ref. 11).

The drive toward smaller, faster devices using less power has led to some radiation sensitivity problems. Single particle upset of flip-flops and RAM's (random access memories) has been discovered in three situations. First, May and Woods (Ref. 12) and Yaney et al, show that ppm U-238 and Th-230 impurities in ceramic packaging materials can yield alpha particles during spontaneous fission which cause soft errors. Second, several groups (References 13, 14, 15, 16) postulate that galactic cosmic rays, particularly the iron group and other massive particles, may cause single particle upset. Third, Guenzer et al (Ref. 7) report that single particle upset takes place approximately once for each 10^8 protons or neutrons per cm^2 traversing a 16K RAM. The upsets may be due to (p, alpha) or n, alpha) reactions. This problem may be intensified in the future as submicron geometries with small switching charges become available. Such devices may be vulnerable to protons and electrons directly.

A survey of future trends in microelectronic memory technology by Vail (Ref. 18) points out that solid-state devices are likely to supplant conventional memories such as magnetic cores, disks, drums, and tapes. The system designer may not be able to use the latter devices much longer because those technologies will be phased out. Vail points out that ECL and TTL technologies are intrinsically hard to space radiation while others such as I^2L, CMOS, CMOS/SOS, magnetic bubbles, and CCD's offer potential hardness against space radiation with further development.

4. OTHER RADIATION EFFECTS

This section discusses a few special topics in radiation effects which could affect certain missions. The topics will be illustrated with quantitative data where available.

Radioactivity

Proton and heavy ion radiation from trapped belts, solar flares, and galactic cosmic radiation can activate some materials in structures and components. The lingering radioactivity is much less than the initiating radiation, but may cause certain problems. For example, a sensor in low earth orbit may be turned off during the few minutes required to traverse the magnetic anomaly in order to avoid saturation from the radiation in that region. However, the radioactivity induced during each passage may increase background noise considerably during the next half hour or more. The severity of the problem depends on the materials and configurations, as well as the sensor and system parameters.

Fluorescence

Charged particles penetrating transparent materials, particularly windows, may generate fluorescent radiation (Ref. 19). Recent work indicates the phenomenon is due to Cerenkov radiation (Ref. 20). The problem is severe for low light level sensors in the uv and visible region. Photomultipliers with uv/visible bialkali photocathodes and visible trialkali cathodes experience count rates above 10^6 sec^{-1} in the South Atlantic anomaly. Shielding the faceplates against electrons up to 4 MeV reduces the count rate by a factor of 10. The rest of the count rate is due to protons with energies above 30 MeV (Ref. 19).

Figure 4-1 shows the fluorescent yield for 2 MeV electrons bombarding a borosilicate clad, pure silica core fiber. The yield peaks at an angle near the maximum expected for Cerenkov emission. The total yield depends on many factors such as fiber diameter, numerical aperture, and source angular distribution. Some estimates of total yield can be made by normalizing computed Cerenkov model spectra to experimental results. Several measurements yield values near 5 X 10^{-16} mW/cm-nm-rad/s for 100 micron fibers. The exciting source was 2 MeV bremsstrahlung. The response was measured at 6000 Angstroms.

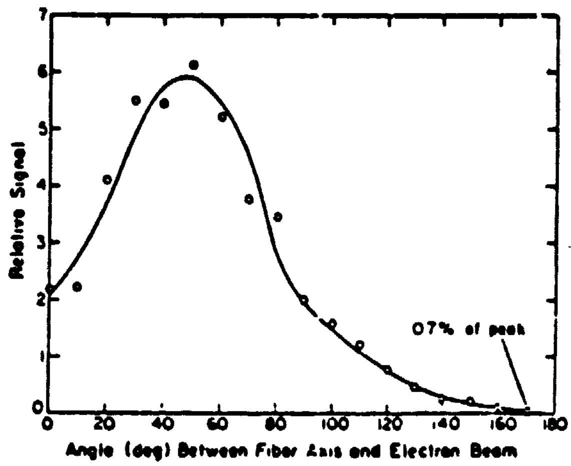

Figure 4-1. Cerenkov Sensitivity per Unit Length

Phosphorescence

The same radiation that causes fluorescence produces defects and dislocations in the crystalline lattice which may produce phosphorescence. The decay constants range from a few minutes to a few days. The intensity of phosphorescent radiation expressed as a fraction of fluorescent intensity ranges from 10^{-2} for some fluorides to 10^{-6} for fused silica (Ref. 6).

Fiber Optics

The use of light pipes or fiber optics as data transmission channels is growing rapidly due to mass, volume, and bandwidth considerations. Mass and volume requirements are reduced, on the average, by a factor of five compared to copper wire cables. Fiber optics have extreme bandwidths; the bandwidth of current fiber optics transmission systems is limited primarily by transmitters and receivers to about 50 MHz. Tests performed by several research laboratories prove that fiber optics bundles can be made to withstand severe mechanical stresses such as crushing, shear, tensile, and vibration, as well as large temperature differentials.

Fiber optics are relatively insensitive to EMP and EMI pickup. In one test, 100-ampere switching transients were present on a copper cable adjacent to a fiber optics cable which suffered no data degradation. On the other hand, ionizing radiation can generate light pulses which may confuse the data stream and cause transmission errors. Such errors could degrade the probability of mission success, but will usually not destroy the system. The basic mechanisms causing luminescence are a subject of debate at present.

Until recently, the utility of fiber optics in system applications was severely limited due to excessive losses in most dielectric materials. Even high quality optical glass exhibits losses on the order of thousands of db's per kilometer. Early fiber optic materials were very susceptible to neugron and gamma radiation. In the late 60's, using fuzed quartz, fibers with losses in the 80 db/km range were developed. In 1970 Corning Glass announced a fiber with a loss of 20 db/km. This startling announcement was followed by another one in 1972 of a 4 db/km fiber. There are presently prototype fibers that exhibit attenuation characteristics of 2 db/km or less.

Each fiber consists of a core of transparent dielectric material surrounded by a cladding material with a lower refractive index than that of the core. Light incident on one end within the acceptance angle will suffer total reflection when it encounters the wall. Loss of transmitted light is due mainly to imperfections in the fiber.

In addition to guidance and control signals, fiber optics can also be used in missile systems to transmit energy. Using compact laser sources, it is possible to detonate electroexplosive devices over fiber optics cables 300 feet long. The potential applications in the areas of motor initiation, thrust vector control systems, and interstage separation systems are only now being explored. The potential weight, volume, low EMP susceptibility, and reliability make the use of fiber optics attractive for these and other applications.

The radiation sensitivity of fiber optics has been studied for several years. The reduction in impurity levels necessary for low loss fiber technology has also reduced the radiation sensitivity of these fibers. Limited data are available on the effects caused by gammas, neutrons, electrons, and protons. The radiation effects of interest are increased optical absorption, fluorescence, and phosphoresence.

<u>Absorption and Fogging</u>

An increase in optical absorption reduces the transmitted signal strength. Radiation can introduce defects into transparent optical material. The defects may create absorption bands, causing a fogging or "browning" of the material. Sapphire and fused silica are relatively insensitive to fogging. The dose range of interest is from 10^4 to 10^9 rads.

Until recently, applications such as hot cell windows, photomultiplier windows, and spacecraft windows were of prime concern and absorption measurements were made at high radiation levels. Table 4-1 shows the effect of 20 megarad to 5000 megarad gamma doses on several glasses at four wavelengths. These radiation levels are too high to be interesting in fiber optics because other system components will fail at lower levels.

Table 4-1. Light Transmission in Optical Materials Subject to Gamma Radiation

Material	Radiation Dose (R)	Average Light Transmission Before Dose (%)	Light Transmission after Dose (%) at Various Wavelengths			
			4000 Å	5000 Å	6000 Å	7000 Å
Purified fused silica (Corning 7940)	5×10^{9}	100	89	89	89	89
Dense flint-2 (617:366)	5 × 10[illegible]	94	0	1	11	21
Dense flint-2 protected (617:366P)	1×10^{9}	91	45	83	85	86
Borosilicate crown-2 (517:645)	1×10^{9}	98	0	3	25	46
Borosilicate crown-2 protected (517:645P)	1×10^{9}	98	60	86	88	89
Vycor	2×10^{7}	99	0	0	0	1
Vycor protected	5×10^{8}	99	24	24	36	61
Quartz	1×10^{9}	99	35	30	31	56
Type 1723 electron-tube envelope glass	1×10^{8}	83	7	23	39	63
Styron 690, [illegible] in. thick	1×10^{9}	65	0	11	47	62
Styron 690, [illegible] in. thick	1×10^{9}	75	0	2	28	56

Tests performed on 4 db/km optical cable show that exposure to 4300 rads (Co-60) increased the attenuation by a factor of 3 (~4 db) and a fluence of 1.4×10^{12} n/cm^2 14 MeV neutrons increased the attenuation by a factor of 5 (~7 db). The length of the cable is not specified. Data transmission systems may be designed to operate at 20 db loss through the transmission medium so that permanent disablement due to optical absorption at these levels is unlikely.

The absorption data presented above were measured over a long time period which permits annealing of the defect centers causing absorption. Transient radiation pulses may cause transient absorption spikes and produce system upset. Evans and Sigel (Ref. 21) have measured permanent and transient radiation-induced losses in several types of optical fibers. They show an induced loss ranging from 10^{-5} to 50 db/km/rad depending on fiber materials, clad materials, and wavelength. Saturation effects are sometimes present so it is not safe to scale down large dose results to the low dose region. Transient attenuation is apparent after pulsed irradiations. Decay time constants range from milliseconds to tens of seconds.

Digicon

A digicon is a sensitive detector of visible or ultraviolet light. Photons incident on the photocathode, shown in Figure 4-1, generate photoelectrons which are accelerated electrostatically and focused magnetically upon a diode array at the other end. The array may contain 1000 diodes or more to provide good resolution of the image. Recent experiments yield estimates of radiation sensitivity for the digicon.

Nabor and Shreve (Ref. 22) irradiated the entry face of a digicon with gamma rays (Cs-137) and electrons (Tl-204). No signal was observed with the accelerating voltage off, so direct effects in the diodes are not significant. The important effect with the voltage on appears to be fluorescence in the faceplate which is converted to photocathode electrons. One diode count is recorded for each 10^5 gammas/cm^2 at the center of the faceplate. Because the diode is 50 X 200 microns, apparently each gamma photon converts to about 0.1 counts. Each Tl-204 electron converts to one count.

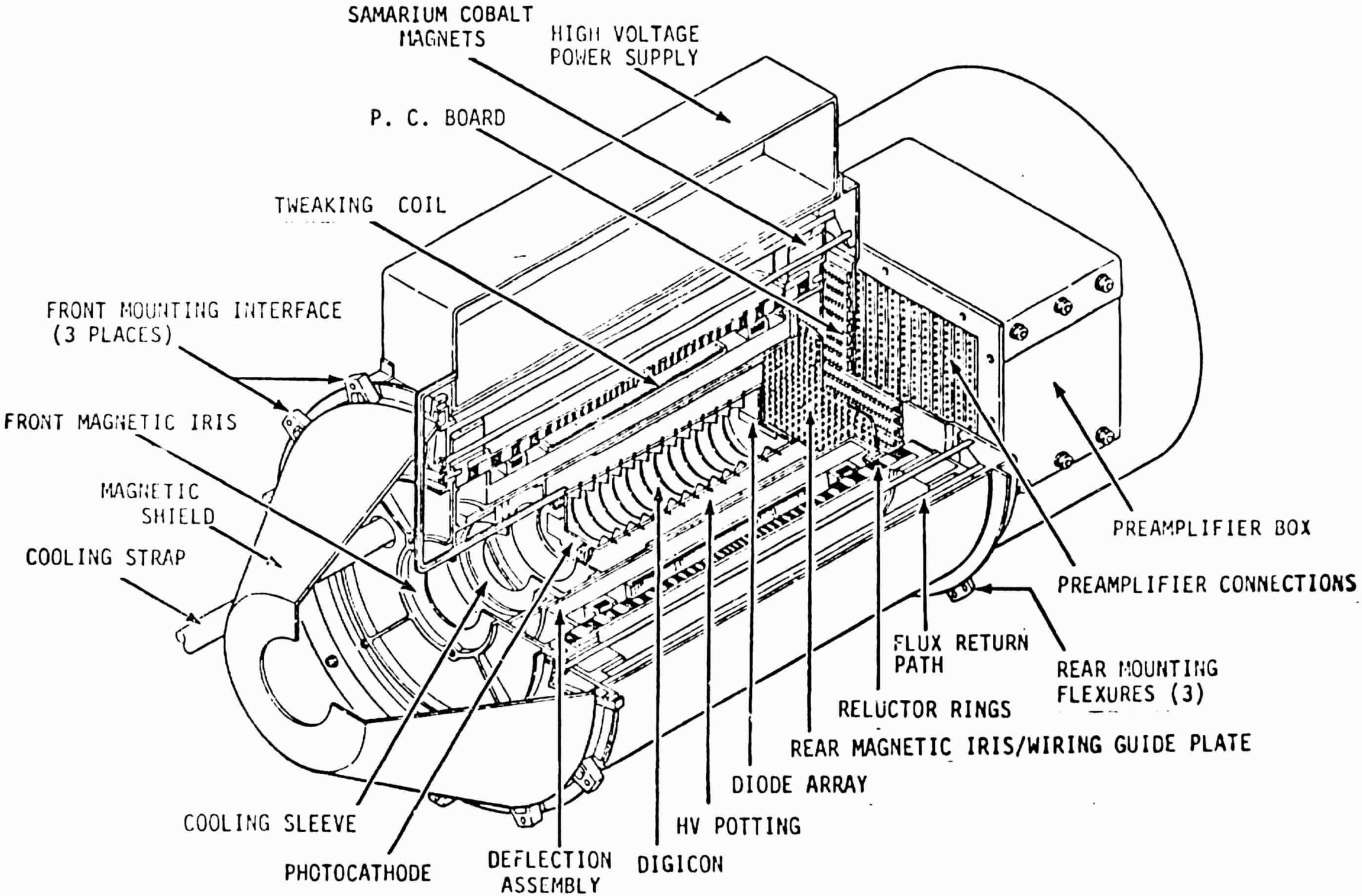

Figure 4-1. Digicon Detector Assembly (from Bell Aerospace)

Dr. Jay Becker (Ref 23) of Old Dominion University reports that 40 MeV protons stimulate the diodes directly. Each proton hitting a diode generates 8 counts, with another 2 to 3 counts arising from fluorescence in the faceplate. The direct diode stimulated counts were observed with the high voltage off. On the other hand, rotation of the digicon by 10 degrees caused the proton beam to miss the diodes. In this case, the directly stimulated counts vanished, but the fluorescent-induced counts persisted.

The data reported in both experiments apply to digicons produced by Science Applications, Inc.

5. REFERENCES

1. Tada, H. Y. and Carter, Jr., J. R.: Solar Cell Radiation Handbook, JPL Pub. 77-56, November 1, 1977.

2. Lindmayer, J. and Allison, J. F.: "The Violet Cell: An Improved Silicon Solar Cell," Comsat Technical Review, Vol 3, No. 1, Spring 1973.

3. Cooley, W. C. and Janda, R. J.: Handbook of Space-Radiation Effects on Solar-Cell Power Systems, NASA SP-3003, 1963.

4. Meulenberg, Jr., A.: "The Sawtooth Cover Slide," Solar Cell High Efficiency and Radiation Damage, NASA CP-2020, May 1977.

5. Wise, J. F.: Silicon Solar Cell, Patent Application Serial No. 579801.

6. Rahilly, W. P.: Vertical Multijunction Solar Cells, Ninth IEEE Photovoltaic Specialists Conference, May 1972.

7. Lindmayer, J.; Wrigley, C.; and Wohlgemuth, J.: Developments in Vertical-Junction Silicon Solar Cells, Solar Cell High Efficiency and Radiation Damage, NASA CP-2020, May 1977.

8. Mandelkorn, J., et al.: Studies of the BSF Cell, NASA TM X-3326, December 1975.

9. Knechtli, R. C., Kamath, S.; and Loo, R.: GaAS Solar Cell Development, Solar Cell High Efficiency and Radiation Damage, NASA CP-2020 May 1977.

10. West, W. S.; Poch, W.; Holmes-Sielde, A.; Bilsky, H. W.; and Carroll, D.: Subsystem Radiation Susceptability Analysis for Deep-Space Missions, NASA TR R-371, November 1971.

11. Myers, D. K.: Ionizing Radiation Effects on Various Commercial NMOS Microprocessors, Annual Conference on Nuclear and Space Radiation Effects, The College of William and Mary of Virginia, Williamsburg, Va., July 12-15, 1977, IEEE Extended Abstracts, Vol. 24A, July 1977.

12. May, T. C. and Woods, M. H.: Alpha-Particle-Induced Soft Errors in Dynamic Memories, IEEE Trans. Electron Devices, ED-26, 1979.

13. Binder, D.; Smith, E.C.; and Holman, A.B.: Satellite Anomalies from Galactic Cosmic Rays, IEEE Trans. Nucl. Sci., NS-22, 1975.

14. Pickel, J. C. and Blandford, J. T.: Cosmic Ray Induced Errors in MOS Memory Cell, IEEE Trans Nucl Sci, NS-25, 1978.

15. Bradford, J. N.: Heavy Ion Radiation Effects in VLSI, RADC-TR-78-109, May 1978.

16. Ziegler, J. F. and Lanford, W. A.: The Effect of Cosmic Rays on Computer Memories, to be published.

17. Guenzer, C. S.; Wolicki, E. A.; and Allas, R. G.: Single Event Upset of Dynamic RAMS by Neutrons and Protons, IEEE Trans. Nucl. Sci., NS-26, 1979.

18. Vail, P. J.: A Survey of Radiation Hardened Microelectronic Memory Technology, IEEE Trans. Nucl. Sci., NS-25, 1978.

19. Viehmann, W., Eubanks, A. G., and Bredekamp, J. H., Fluorescence and Phosphorescence of Photomult‹plier Window Materials Under Irradiation, NASA TR R-70695, Preprint X-755-74-219, July 1974.

20. Golob, J. E., Lyons, P. B., and Looney, L. D., Transient Radiation Effects in Low Loss Optical Waveguides, LA-UR-77-1564, Annual Conference on Nuclear and Space Radiation Effects, The College of William and May of Virginia, Williamsburg, Va., July 12-15, 1977, IEEE Extended Abstracts, Vol. 24A, July 1977.

21. Sigel, Jr., G. H. and Evans, B. D.: IEEE Trans. Nucl. Sci., NS-22, p 2462, 1975. Also Friebele, E.J.; Jaeger, R.E.; Sigel, Jr., G.H.; and Gingerich, M.E.: Effect of Ionizing Radiation on the Optical Attenuation in Polymer-Clad Silica Fiber-Optic Waveguides, Appl. Phys. Lett. 32 (2), 15 January 1978.

22. Armstrong, T.; Hill, C.; Colborn, B.; Nabor, J.; and Shreve, D.: Study of Particle Radiation and Shielding for the High-Resolution Spectrograph Aboard the Space Telescope, Science Applications, Inc., Report, to be published.

23. Dr. Jay Becker, Old Dominion University, private communication.